J. Mech. Phys. Solids 158 (2022) 104675

Contents lists available at ScienceDirect

Journal of the Mechanics and Physics of Solids

journal homepage: www.elsevier.com/locate/jmps

Polyacrylamide hydrogels. IV. Near-perfect elasticity and rate-dependent toughness

Sammy Hassan [1], Junsoo Kim [1], Zhigang suo [*]

John A. Paulson School of Engineering and Applied Science, Kavli Institute for Nanobio Science and Technology, Harvard University, Cambridge, MA 02138, United States

ARTICLE INFO

Keywords:
Rate-dependency
Polyacrylamide
Toughness
Hydrogels
Sliding stress

ABSTRACT

A polyacrylamide hydrogel exhibits near-perfect elasticity: its stress-stretch curve is rate-independent and has negligible hysteresis. The near-perfect elasticity results from the large amount of water between the polymer chains. Water has low viscosity and lubricates polymer chains. Here we report that the polyacrylamide hydrogel exhibits rate-dependent toughness when the polymer chains are long. We interpret this finding as follows. Toughness is measured by rupturing a hydrogel containing a precut crack. When the hydrogel is stretched, at the crack tip, some polymer chains slide relative to others. Before a polymer chain breaks, high tension is distributed over a long length of the chain. Breaking the chain releases the energy stored in the long length of the chain. It is this deconcentration of tension that toughens the hydrogel. When the hydrogel is stretched at a high rate, however, the polymer chain at the crack tip does not have time to slip fully, so that the high tension only transmits over a short segment of the chain. Breaking the chain will lead to a lower toughness. Consequently, the toughness decreases as the stretch rate increases. We invoke a shear lag model and find that the toughness scales with stretch rate as $G_c \sim (\mathrm{d}\lambda/\mathrm{d}t)^{-1/4}$.

1. Introduction

Properties of materials are commonly measured as functions of temperature, T and stretch rate R. For example, in a polymer, the modulus measured as a function of temperature, $E(T, R)$, collapses to a single curve, $E(R/a_T)$, a_T is a function of temperature (Williams et al., 1955). In elastomers, the strength measured as a function of temperature and stretch rate, $s_c(T, R)$, similarly collapses to a single curve, $s_c(R/b_T)$, where b_T is a function of temperature (Smith, 1958). Also in elastomers, the toughness measured as a function of temperature and stretch rate, $G_c(T, R)$ collapses to a single curve, $G_c(R/c_T)$, where c_T is a function of temperature (Mullins, 1959). Even though a_T, b_T, and c_T are somewhat different functions of temperature, these observations have been taken as evidence that all these properties are rate-dependent through the same kinetic process: viscoelasticity.

We have recently studied a polyacrylamide hydrogel of dense entanglements and long chains (Kim et al., 2021). The stress-stretch curve is nearly rate-independent. This near-perfect elasticity of highly swollen hydrogels results from the low viscosity of water. In the present paper, we show that strength, as well as modulus, of the hydrogel is rate-independent. However, toughness drops by a factor of three when the stretch rate changes from 0.00035 s^{-1} to 1.1 s^{-1}. We interpret these experimental findings as follows. The modulus and

* Corresponding author.
E-mail address: suo@seas.harvard.edu (Z. suo).
[1] These authors equally contributed to this work.

https://doi.org/10.1016/j.jmps.2021.104675
Received 10 July 2021; Received in revised form 8 October 2021; Accepted 8 October 2021
Available online 14 October 2021

strength are measured using a sample without a precut crack, where the deformation is nearly affine, involving little relative sliding between polymer chains. Consequently, the low viscosity of water makes the modulus and strength nearly rate-independent. The toughness is measured using a sample containing a precut crack, where the deformation is non-affine, involving large relative sliding between polymer chains. When the hydrogel is stretched, at the crack tip a polymer chain slides relative to other chains. The relative sliding causes a sliding stress on the chain through the viscosity of water. Consequently, the toughness is rate-dependent.

We further introduce a model that explains why the toughness of the hydrogel decreases as stretch rate increases (Fig. 1). When the hydrogel is stretched, a polymer chain at the crack tip pulls out before breaking, sliding against other polymer chains in the hydrogel. The sliding causes stress on the polymer chain through the viscosity of water. When the stretch rate is low, the sliding stress is negligible. Before the chain breaks, tension transmits over the entire length of the chain. When the chain breaks at a single covalent bond, the energy of the entire chain is released, leading to high toughness. This picture of the de-concentration of tension is attributed to Lake and Thomas (Lake and Thomas, 1967). The de-concentration of tension relies on the fundamental nature of a polymer network: the covalent bonds along a polymer chain are much stronger than the noncovalent interaction between polymer chains. In the Lake-Thomas picture, the interaction between the polymer chains is completely neglected. The original Lake-Thomas picture, however, is inconsistent with our experimental observation that toughness is rate-dependent. We modify the Lake-Thomas picture by including the interaction between the polymer chains. When the stretch rate is high, the sliding stress is large. Before a polymer chain breaks at the crack tip, tension transmits over a short segment of the chain. Breaking the polymer chain releases the energy stored in the short segment, leading to low toughness. We represent this modified Lake-Thomas picture by a shear lag model and find that the toughness scales with stretch rate as $G_c \sim (d\lambda/dt)^{-1/4}$, where $d\lambda/dt$ is global stretch rate.

2. Experiments

2.1. Preparation of two types of hydrogels

Following (Kim et al., 2021), we synthesize a highly entangled, long-chain hydrogel. The precursor of the polyacrylamide hydrogel consists of acrylamide (AAm, A8887), N,N'-methylenebisacrylamide (MBAA, M7279), Irgacure 2959 (photoinitiator, 410,896), and deionized water. All chemicals are purchased from Sigma-Aldrich without modification. We dissolve 30 g of AAm in 15 g of water to obtain a 66.7% AAm solution by weight. We dissolve 0.925 g of MBAA in 60 g of water to obtain 0.1 M MBAA solution. We dissolve 0.224 g of photoinitiator in 10 g of ethanol to obtain 0.1 M photoinitiator solution. When AAm precipitates at room temperature, we heat the solution slightly above room temperature before use. We mix 53.6 mL of AAm solution, 60.3 μL of MBAA solution, 24.1 μL of the photoinitiator solution, and 0.23 mL of water to prepare the precursor. We pour the precursor into a mold consisting of an acrylic substrate and a rubber spacer, and cover them with a glass plate. We apply ultraviolet light (365 nm, ~ 1.5 mW/cm^2) for 3 h to polymerize and crosslink. The cured hydrogel is demolded and immersed in water for one day to swell to equilibrium. We synthesize a short-chain hydrogel by mixing 53.4 mL of AAm solution, 500.5 μL of MBAA solution, and 300.3 μL of photoinitiator solution to prepare the precursor. The cured hydrogel is demolded and also immersed in water for one day to swell to equilibrium.

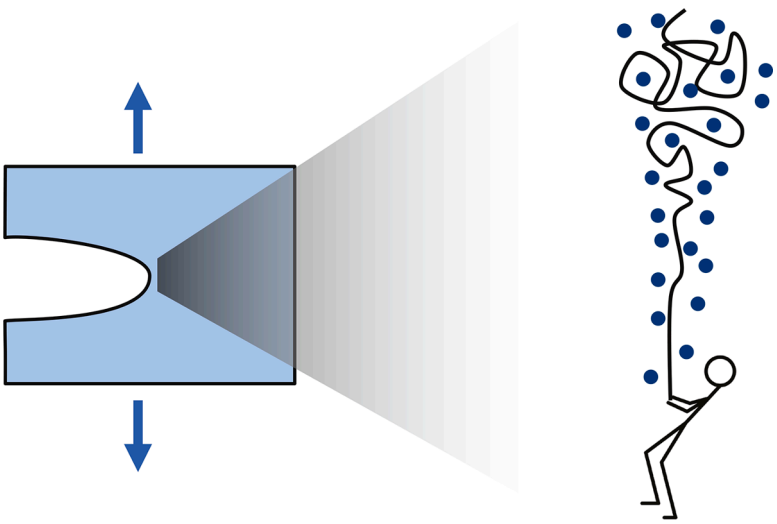

Fig. 1. A schematic of a polymer chain pulled out of a hydrogel, near a crack tip, at a large stretch rate. The polymer chain slides against other polymer chains in the hydrogel. A sliding stress, due to the water molecules, acts on the polymer chain and concentrates tension into a short segment of the chain.

2.2. Stress-stretch curves

We prepare a thin rectangular sheet of a hydrogel and fasten its ends to two rigid clamps. The gel undergoes one cycle of loading and unloading, and the force is recorded. The stretch, λ is defined by the height of the sample in deformed state divided by the height of the sample in the reference state. We perform the experiment in stretch rates ranging from 0.00035 s^{-1} to 1.1 s^{-1}, and plot the stress-stretch curve for each stretch rate (Fig. 2a). The stress-stretch curves are nearly identical. The modulus is calculated from the initial slope (stretch: 1 ~ 1.05) of the stress-stretch curves, and is independent of rate (Fig. 2b). We calculate the hysteresis at each stretch rate by dividing the area between the loading and unloading curve by the area beneath the loading curve. Our results confirm that the hysteresis of a polyacrylamide hydrogel is small (Fig. 2c). The source of larger scatters in hysteresis at lower stretch rates are uncertain at this writing. Nonetheless, the values of hysteresis measured for all stretch rates are below ~0.03. For a sample without a precut crack, the deformation is nearly affine: the stretch causes little relative sliding between the polymer chains. Because of the low viscosity of water, the hysteresis in a nearly affine deformation is too small to be observed experimentally. By contrast, the as-prepared hydrogel before swelling has a small amount of water and exhibits pronounced hysteresis (Kim et al., 2021).

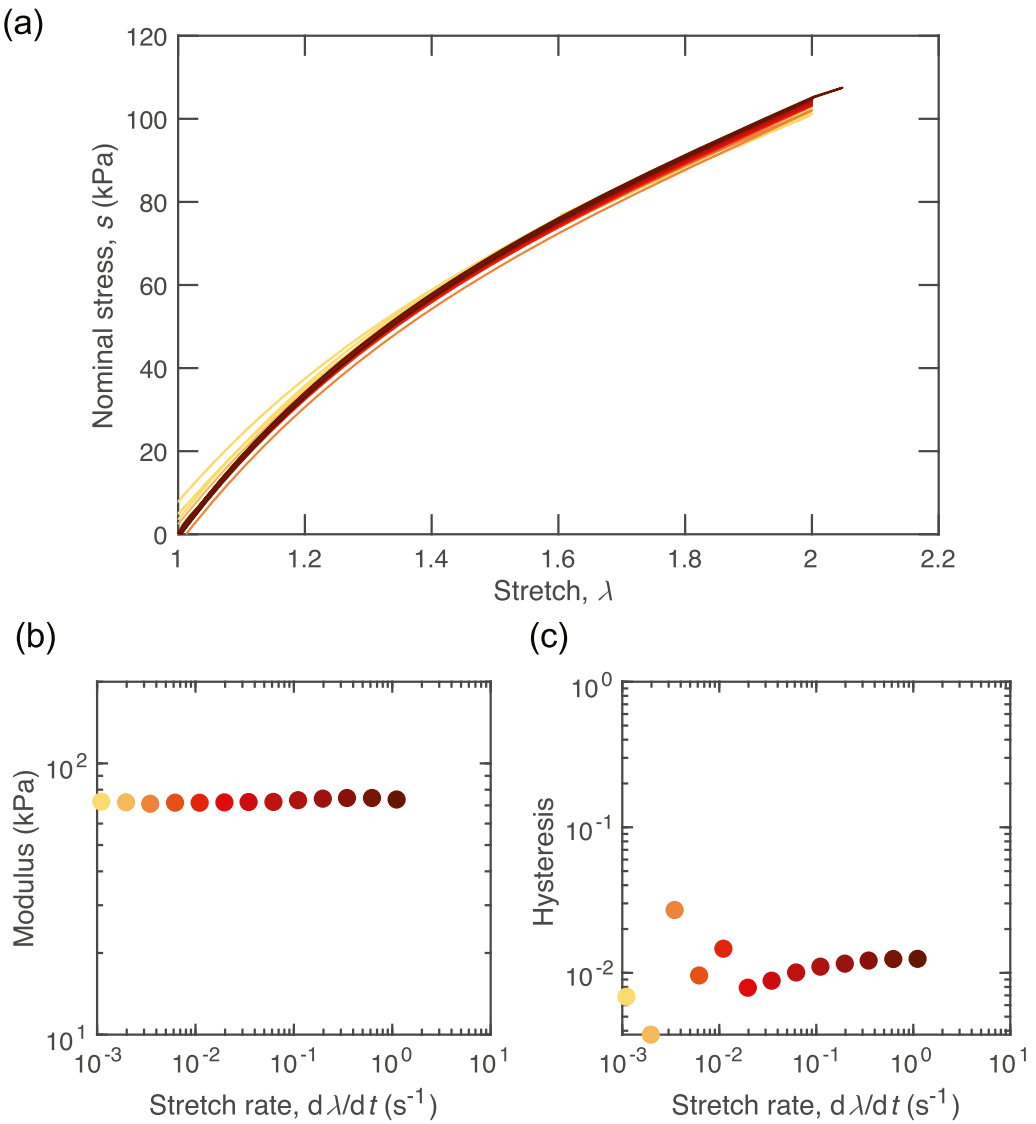

Fig. 2. Rate-independent deformation of samples without precut cracks. (a) Loading unloading curves of the hydrogel at different stretch rates ranging from 0.00035 s^{-1} to 1.1 s^{-1}. Different colors correspond to different stretch rates. (b) Modulus of the hydrogel as a function of stretch rate. (c) Hysteresis of the hydrogel as a function of stretch rate. Each color represents the same stretch rate in all plots.

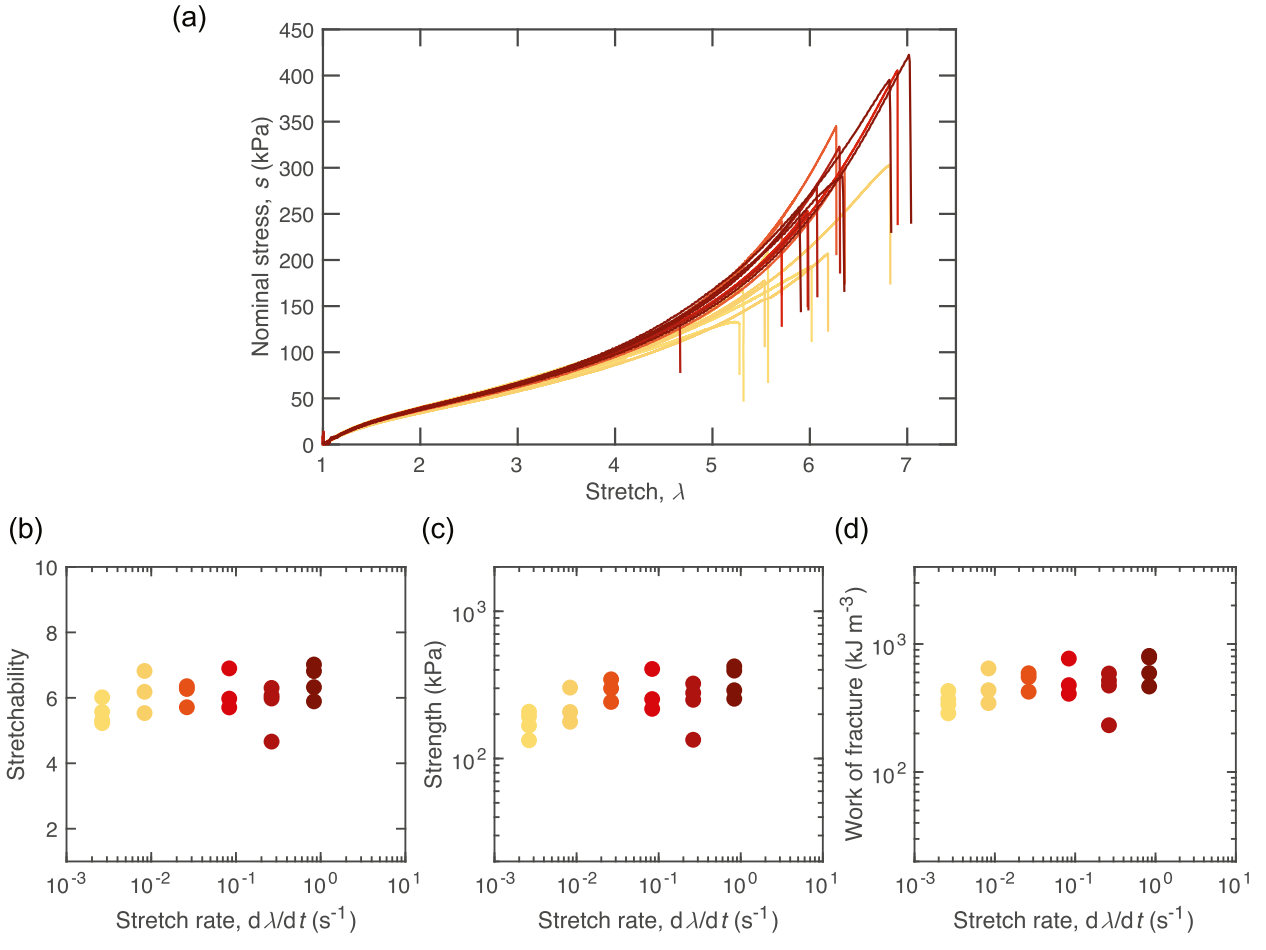

Fig. 3. Rate-independent stretchability, strength, and work of fracture. (a) The stress-stretch curves of the hydrogel until break at different stretch rates ranging from 0.0026 s^{-1} to 0.83 s^{-1}. Different colors correspond to different stretch rates. For each stretch rate, three to five samples are tested. (b) The stretchability of the hydrogel as a function of stretch rate. (c) The strength of the hydrogel as a function of stretch rate. (d) The work of fracture of the hydrogel as a function of stretch rate. Each color represents the same stretch rate in all plots.

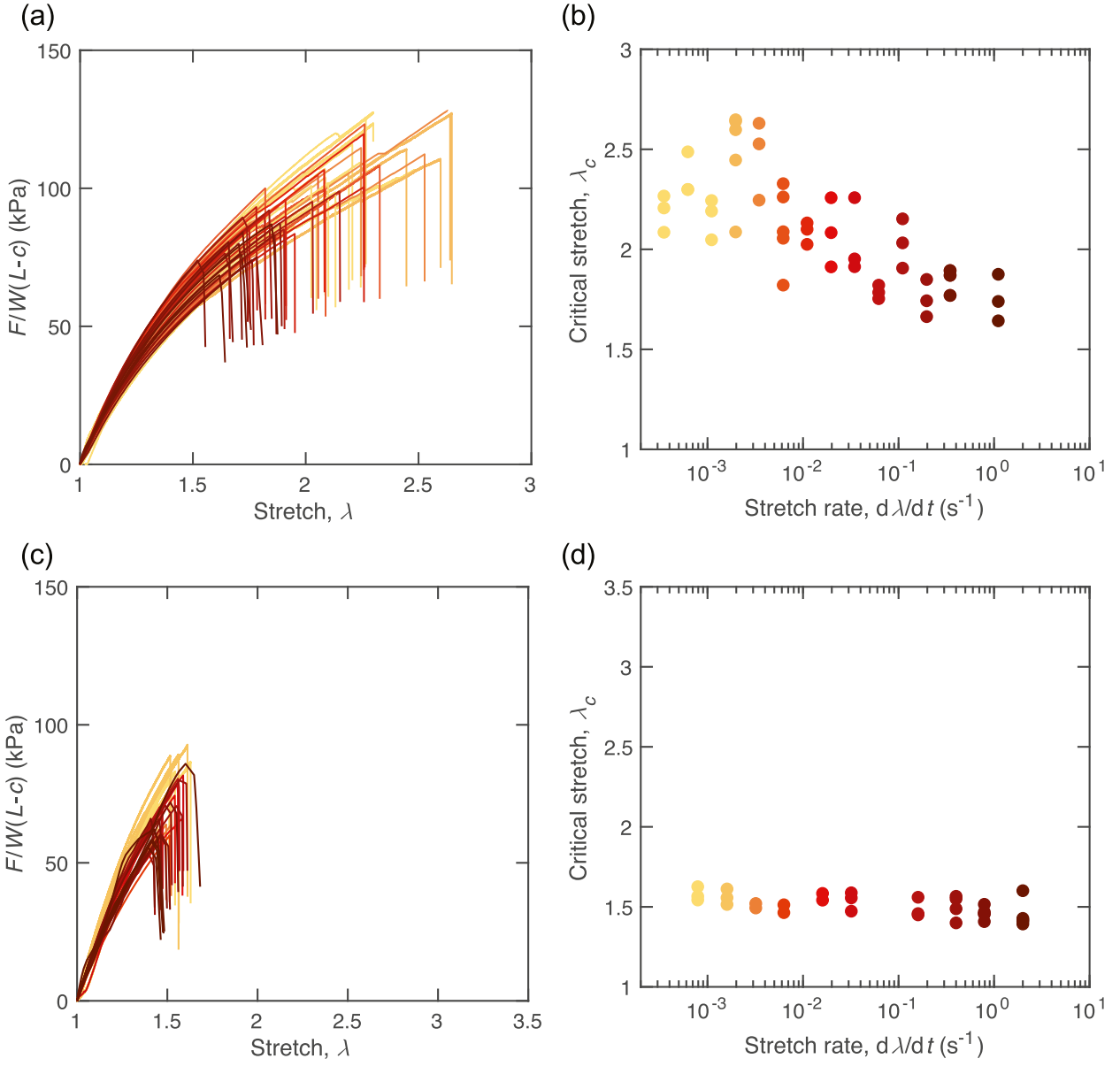

Fig. 4. Force-stretch curves of samples with precut cracks. (a) The force-stretch curves of the hydrogel at different stretch rates ranging from 0.00035 s^{-1} to 1.1 s^{-1}. Different colors correspond to different stretch rates. (b) The critical stretch of the hydrogel as a function of stretch rate. (c) The force-stretch curves of the short-chain hydrogel at different stretch rates ranging from 0.00035 s^{-1} to 2.0 s^{-1}. (d) The critical stretch of the short-chain hydrogel as a function of stretch rate. Each color represents the same stretch rate in all plots.

2.3. Strength, stretchability, and work of fracture

We cut the hydrogel into a dumbbell-shaped specimen, and measure its strength at stretch rates ranging from 0.0026 s^{-1} to 0.83 s^{-1}. To display statistical variation from sample to sample, three to four samples are measured for each stretch rate (Fig. 3a). The stress-stretch curves until rupture vary somewhat from sample to sample, but are independent of stretch rate. The same is true for stretchability (Fig. 3b) and strength (Fig. 3c). The work of fracture at each stretch rate is given by the area beneath the stress-stretch curve until rupture. The work of fracture also varies from sample to sample, but is independent of stretch rate (Fig. 3d). We again attribute the rate-independent stretchability, strength, and work of fracture to the little relative motion between chains during deformation, as well as the low viscosity of water.

2.4. Toughness

Following (Rivlin and Thomas, 1953), we introduce a precut crack into a thin rectangular sheet of a hydrogel, clamp its long edges, and stretch the sheet until the crack propagates. The tensile tester records the applied force as a function of the stretch. We divide the force by $W(L\text{-}c)$, where W is the thickness of the sample, L is the length of the sample, and c is the length of the pre-cut crack, and plot it as a function of stretch at different stretch rates (Fig. 4a). The stretch, λ, is again defined by the height of the sample in deformed state divided by the height of the sample in the reference state. The experiments are conducted using multiple samples at stretch rates ranging from 0.00035 s^{-1} to 1.1 s^{-1}. At each fixed stretch rate, the experiment is repeated three to five times, and the stretch at rupture, λ_c, varies from sample to sample (Fig. 4b). Furthermore, λ_c decreases as the stretch rate increases.

Next, we synthesize a hydrogel of short polymer chains, submerge it in water to swell to equilibrium, add a precut crack, and stretch each sample until rupture. We obtain the force-stretch curves at stretch rates ranging from 0.00035 s^{-1} to 2.0 s^{-1} (Fig. 4c). Unlike the long-chain hydrogel, the force-stretch curves of the short-chain hydrogel with a precut crack are independent of stretch rate (Fig. 4d).

As noted before, the stress-stretch curves of samples without precut cracks are nearly independent of stretch rate (Fig. 2a). For a sample without a precut crack, the area under its stress-stretch curve up to a stretch, λ, defines the elastic energy per unit volume in the sample, $W(\lambda)$. When a sample with a precut crack ruptures at stretch λ_c, the toughness is $G_c = HW(\lambda_c)$, where H is the height of the sample in the undeformed state. We plot the toughness of both long-chain hydrogel and short-chain hydrogel as functions of stretch rate (Fig. 5). For the long-chain hydrogel, at low stretch rates the toughness plateaus, but at high stretch rates, the toughness decreases with the stretch rates. Our data at high stretch rates fit to a power law, $G_c \sim (\mathrm{d}\lambda/\mathrm{d}t)^{-1/4}$. For the short-chain hydrogel, the toughness is nearly independent of stretch rate.

3. Model

We interpret the various experimental observations as follows. For samples of the long-chain hydrogel without precut cracks, the stress-stretch curve (including stretchability, strength, and work of fracture) is nearly rate-independent (Fig. 3). This near-perfect elasticity results from two factors: the low viscosity of water, and near affine deformation of samples without precut cracks.

For samples of the long-chain hydrogel with precut cracks, the critical stretch decreases as the stretch rate increases (Fig. 4b). The data let us plot toughness as a function of stretch rate (Fig. 5). The toughness plateaus at low stretch rates, but decreases at high stretch rates. We interpret this behavior by a generalization of the Lake-Thomas model (Lake and Thomas, 1967). When the hydrogel is

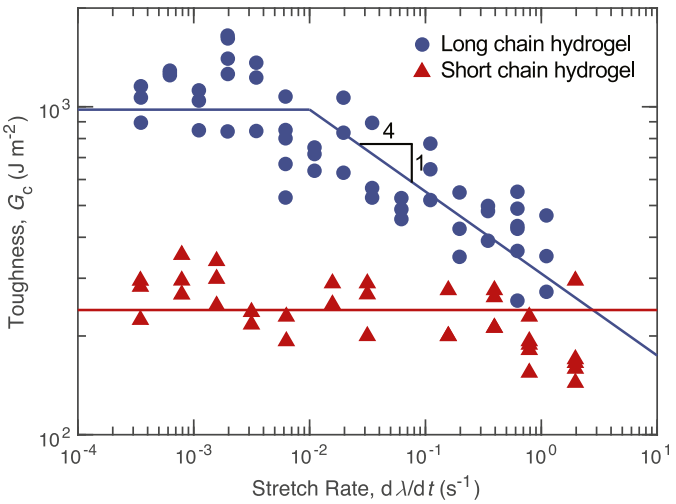

Fig. 5. The toughness of the long-chain hydrogel and the short-chain hydrogel as a function of stretch rate. The toughness of the long-chain hydrogel is constant at low stretch rates and decreases beyond a stretch rate of 10^{-2}. At high stretch rates, toughness scales with stretch rate as $G_c \sim (\mathrm{d}\lambda/\mathrm{d}t)^{-1/4}$. The toughness of the short-chain hydrogel is rate-independent at all stretch rates tested in the work.

stretched, at the crack tip a polymer chain slides relative to other chains. The relative sliding causes a sliding stress on the chain through the viscosity of water (Fig. 1). As the polymer chain pulls out of the hydrogel, the sliding stress balances the tension in the polymer chain. At low stretch rates, the sliding stress is negligible, and tension distributes evenly along the entire length of the polymer chain. When the chain breaks at a single covalent bond, the energy of the entire chain is released, leading to high toughness. Consequently, at low stretch rates toughness is independent of stretch rate, as pictured in the Lake-Thomas model. We identify the plateau toughness at low stretch rates (Fig. 5) as the value predicted by the Lake-Thomas model (Kim et al., 2021). At high stretch rates, the sliding stress is high, and tension is concentrated within a short segment of the polymer chain. Breaking the polymer chain releases the energy stored in the short segment, leading to low toughness. Consequently, at high stretch rates toughness decreases as the stretch rate increases. This interpretation is corroborated by the observation that the toughness of short-chain hydrogels is nearly independent of stretch rate (Fig. 5). Several studies have suggested poroelastic effects on crack growth in hydrogels (Naassaoui et al., 2018; Noselli et al., 2016; Wang and Hong, 2012; Yalin et al., 2018). The experiments reported in this paper, however, are not designed to test the significance of poroelasticity. We hope to design experiments to study the effect of poroelasticity on fracture in a subsequent paper.

We next develop a model to account for the specific scaling observed in our experiment of the long-chain hydrogel at high stretch rates, $G_c \sim (d\lambda/dt)^{-1/4}$. The model draws upon our previous work on a composite of elastic fibers and elastic matrix with viscous interfaces (Lavoie et al., 2021). We picture a hydrogel as a fiber-matrix composite (Fig. 6). In the hydrogel, consider a plane through which a crack will propagate. A polymer chain that bridges the crack is pictured as a fiber, and the neighboring chains that do not bridge the crack are pictured as a matrix. Surrounding the crack-bridging polymer chain is a layer of water, which sets the sliding viscosity.

Let λ_b be the stretch at which the polymer chain breaks, so that the time for the polymer chain to break scales as $t_b \sim \lambda_b(d\lambda/dt)^{-1}$. As the polymer chain pulls out from the hydrogel, the pulling force is balanced by the tension in the chain, as well as the sliding stress (Fig. 6b). Because of the sliding stress, the tension is not evenly distributed along the polymer chain, but decreases along the length of the chain. This behavior is called shear lag (e.g., Cox, 1952; Hui et al., 2018; 2020; Lagoudas et al., 1989; Wang et al., 2020). The shear lag with viscous interface leads to a diffusion equation, so that, right before the polymer chain breaks, high tension is developed in a segment of the chain of a length scaled as $L_b \sim t_b^{1/2}$ (Lavoie et al., 2021). When the polymer chain breaks, the elastic energy stored in this segment is released. For a polymer chain, $L_b = bN_b$, where b is the length of a monomer and N_b is the number of monomers that experience high tension. According to the Lake-Thomas model, the toughness scales as $G_c \sim N_b^{1/2}$. The original Lake-Thomas model assumed no sliding stress, so that tension is evenly distributed over the full length of the polymer chain. Here we have modified the Lake Thomas model by replacing the full length of the polymer chain with the length of the segment that carries high tension. A combination of the above three scaling relations leads to $G_c \sim (d\lambda/dt)^{-1/4}$.

The original Lake-Thomas model is only applicable when the length of the high-tension segment is comparable to the full length of the chain. Indeed, the Lake-Thomas model assumes that upon fracture, the elastic energy stored along an entire polymer chain is released, independent of stretch rate. For a long polymer chain, the Lake-Thomas limit is only attained at low stretch rates, where the sliding stress is low. At faster stretch rates, the high-tension segment is shorter than the length of the chain, and the Lake-Thomas model does not hold. For a short polymer chain, the Lake-Thomas limit is attainable at a wide range of stretch rates.

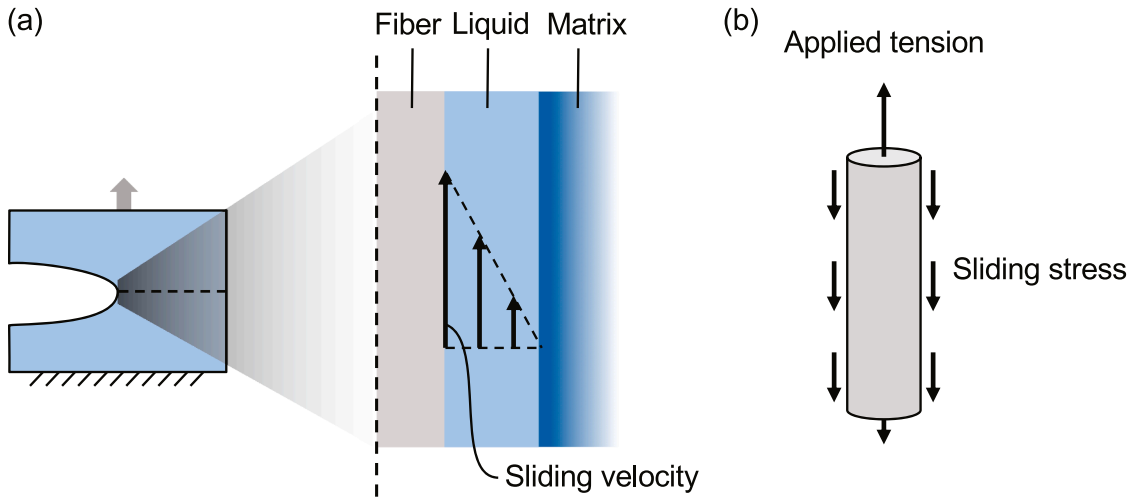

Fig. 6. Modeling stress deconcentration. (a) The hydrogel in the presence of a crack is modeled as a composite consisting of a fiber, a liquid layer, and a matrix. The fiber, liquid, and matrix represent a bridging polymer chain, water molecules, and surrounding polymer chains, respectively. The relative velocity profile in the liquid layer is assumed to be linear, and the sliding stress is taken to be proportional to the relative velocity. (b) Free body diagram of a polymer chain bridging the crack. The applied tension at any point of the polymer chain is balanced by the tension in the chain and the sliding stress.

4. Conclusion

We have shown that while the deformation and strength of a long-chain polyacrylamide hydrogel are rate-independent, the toughness decreases as the stretch rate increases. We have explained this behavior by the sliding of polymer chains at the crack tip. When the hydrogel with a precut crack is stretched at a high rate, the polymer chain at the crack tip does not have time to slip fully, and the high tension only transmits over a short segment of the chain. We modified the Lake-Thomas model to include the effect of stretch rate and find that the toughness scales as $G_c \sim (d\lambda/dt)^{-1/4}$, which agrees with our experimental results.

Declaration of Competing Interest

The authors declare no conflict of interest.

Acknowledgments

This work was supported by MRSEC (DMR-2011754). J.K. acknowledges financial support from the Kwanjeong Educational Foundation.

References

Cox, H.L., 1952. The elasticity and strength of paper and other fibrous materials. Br. J. Appl. Phys. 3, 72–79.
Hui, C.-Y., Liu, Z., Minsky, H., Creton, C., Ciccotti, M., 2018. Mechanics of an adhesive tape in a zero degree peel test–Effect of large deformation and material nonlinearity. Soft Matter 14, 9681–9692.
Hui, C.Y., Liu, Z., Phoenix, S.L., King, D.R., Cui, W., Huang, Y., Gong, J.P., 2020. Mechanical behavior of unidirectional fiber reinforced soft composites. Extreme Mech. Lett. 35, 100642.
Kim, J., Zhan, G., Shi, M., Suo, Z., 2021. Fracture, fatigue, and friction of polymers in which entanglements greatly outnumber crosslinks. Science 374 (6564), 212–216.
Lake, G., Thomas, A., 1967. The strength of highly elastic materials. Proc. R. Soc. Lond. 300, 108–119.
Lagoudas, D.C., Hui, C.-Y., Phoenix, S.L., 1989. Time evolution of overstress profiles near broken fibers in a composite with a viscoelastic matrixAuthor links open overlay panel. Int. J. Solids Struct. 25, 45–66.
Lavoie, S.R., Hassan, S., Kim, J., Yin, T., Suo, Z., 2021. Toughness of a composite in which sliding between fibers and matrix is rate-sensitive. Extreme Mech. Lett. 46, 101317.
Mullins, L., 1959. Rupture of rubber. IX. Role of hysteresis in the tearing of rubber. Trans. Inst. Rubber Ind. 35, 213–222.
Naassaoui, I., Ronsin, O., Baumberger, T., 2018. A poroelastic signature of the dry/wet state of a crack tip propagating steadily in a physical hydrogel. Extreme Mech. Lett. 22, 8–12.
Noselli, G., Lucantonio, A., McMeeking, R.M., DeSimone, A., 2016. Poroelastic toughening in polymer gels–A theoretical and numerical study. J. Mech. Phys. Solids 94, 33–46.
Rivlin, R., Thomas, A.G., 1953. Rupture of rubber. I. Characteristic energy for tearing. J. Polym. Sci. 10, 291–318.
Smith, T.L., 1958. Dependence of the ultimate properties of a GR-S rubber on strain rate and temperature. J. Polym. Sci 32, 99–113.
Wang, Y., Yang, X., Nian, G., Suo, Z., 2020. Strength and toughness of adhesion of soft materials measured in lap shear. J. Mech. Phys. Solids 143, 103988.
Wang, X., Hong, W., 2012. Delayed fracture in gels. Soft Matter 8, 8171–8178.
Williams, M.L., Landel, R.F., Ferry, J.D., 1955. The temperature dependence of relaxation mechanisms in amorphous polymers and other glass-forming liquids. J. Am. Chem. Soc. 77, 3701–3707.
Yalin, Y., Landis, C.M., Rui, H., 2018. Steady-state crack growth in polymer gels–A linear poroelastic analysis. J. Mech. Phys. Solids 118, 15–39.